STRUCTURAL AND DIFFUSION WEIGHTED MRI REGISTRATION FOR BIOMARKER FUSION IN CROHN'S DISEASE DIAGNOSIS

Vahid Taimouri, Sila Kurugol, Sean Clancy, Moti Freiman, Simon K. Warfield

Computational Radiology Laboratory, Department of Radiology, Boston Children's Hospital, Harvard Medical School, Boston, Massachusetts, USA

ABSTRACT

Diffusivity of water molecules estimated from diffusion weighted MRI (DW-MRI) is an important biomarker to pinpoint regions with restricted diffusion such as inflamed bowel regions in patients with Crohn's Disease (CD). There is a need to fuse the information extracted from DW-MRI with other image modalities, e.g. structural T1w images, for more accurate and efficient diagnosis. However, due to low signal-to-noise ratio, distortion and lower resolution of DW-MR images compared to T1w images, fusion of these image modalities is challenging, especially in turns and folds of the bowel. This paper presents a novel method to register structural T1w and diffusion weighted images, which facilitates the image fusion. Based on the block-matching algorithm, the proposed method first determines multiple candidate matches in a neighborhood, and then iteratively finds the most probable match using additional geometric information. We examined the performance of the proposed method on five patients with confirmed CD. Our method outperformed other state-of-the-art registration methods, i.e. ANTS and Demons. This method has the potential for being a useful tool in structural and DW-MRI data fusion for more accurate CD diagnosis and severity assessment.

***Index Terms*—** Diffusion weighted imaging, Image registration, Abdomen imaging, Crohn's Disease

1. INTRODUCTION

Crohn's Disease (CD) is a chronic, relapsing and remitting inflammatory bowel disease [1]. Magnetic resonance imaging is commonly used for imaging Crohn's Disease in clinical practice because of its lack of ionizing radiation and good tissue contrast. However, assessment of inflammatory activity requires acquisition of T1w images after gadolinium IV contrast injection, which can be associated with rare but severe complications [2]. Instead, quantitative diffusion-weighted MR imaging (DW-MRI) [1] has been suggested for detection of inflammatory activity in CD [3]. Parameters estimated from DW-MRI images using either a single exponential decay model or more complex and accurate models of diffusion signal have been shown to be useful biomarkers for CD activity assessment [4, 5].

Despite providing useful markers to the clinicians, DW-MRI images and parametric maps are not utilized very often in clinical practice due to the difficulty of immediately locating the same bowel section and inflamed area in both structural MRI and DW-MRI images. This is due to a lack of registration methods between high-resolution structural images and lower-resolution DW-MRI images.

Recently, Erdt *et al.* studied the DW-MRI to structural MRI registration problem for liver regions [6]. However, the registration of DW-MRI and structural data in the bowel imposed some specific challenges, including: 1. The enhanced and non-enhanced regions in DW-MRI images causing intensity inhomogeneity; 2. Anisotropy of DW-MRI voxel size, e.g. $1.98\times1.98\times5mm^3$; 3. Non-rigid deformation of the bowel, especially when the bladder enlarges in post-contrast structural image, due to administration of oral contrast which results in anatomic deformation between the DWI and structural images in the abdomen (Fig. 1).

In this work, we address the challenging task of abdomen and bowel registration by introducing a novel registration method which is based on the Block-Matching Algorithm (BMA). Our method chooses the most probable matching between blocks from the reference and target images, using both intensity and geometric information, and produces reliable registration. Our algorithm enables the clinicians to interpret images from multiple sequences, and to fuse disease markers from each sequence (such as amount of bowel wall thickening and change in DW-MRI parameters) for quantitative assessment of disease severity in clinical practice.

(a) (b)

Fig. 1. (a) The structural T1w, and (b) the DWI image (b=100 s/mm^2) from the coronal view show the bladder (identified by the red dashed arrows) and the enhanced bowel wall (identified by the green arrows) which causes contrast inhomogeneity.

2. MATERIALS AND METHODS

2.1. Data acquisition

MR enterography (MRE) data and DW-MRI data were acquired from five Crohn's disease patients using a standard clinical acquisition protocol with a 1.5-T scanner (Magnetom Avanto, Siemens Medical Solutions, Erlangen, Germany). The MRE protocol for these patients included administration of polyethylene glycol for bowel distention prior to acquisition. The protocol included acquisition of axial DW-MRI with a free-breathing single-shot echo-planar imaging with an in plane resolution of 1.8 mm, slice thickness of 5mm and TE/TR of 77/7500 ms; 7 b-values = 0, 50, 100, 200, 400, 600, 800 s/mm^2 with 1 excitation.

As part of the protocol, 3D T1 weighted coronal gradient recalled echo sequence were acquired with a volume-interpolated breath hold exam (VIBE) before and after administration of gadolinium-containing contrast agent with an in-plane resolution of 0.7mm, slice thickness of 2mm and TE/TR of 1.35/3.77ms. The acquisition time was 16.66 sec. An enhancing region of bowel wall in the ileum was labeled manually by an expert to define the region of interest (ROI) on both DW-MRI data (b-value equals 800 s/mm^2) and coronal T1-weighted data of each patient using the ITKSNAP software tool [7].

2.2. DWI-T1w registration method

The registration method is based on the Block-Matching Algorithm, which aims at bringing the corresponding anatomical locations in two images into alignment, especially in the bowel. In the standard BMA [8], the best match with the highest similarity score value in the neighborhood is chosen as the true match; however, due to the bowel shape and length as well as the existence of several bowel folds nearby, there might be several matches with high similarity score values. Therefore, the highest similarity score value does not necessarily result in correct anatomical match identification. To circumvent this problem, we preserve all the candidate matches in a neighborhood to identify the most probable match using additional geometric information along with the similarity scores with an iterative method.

Specifically, we first calculate a similarity value (scc$_j$) between each block centered at voxel *m* in the target structural image (**M**) and each block centered at voxel *j* in a neighborhood $\mathcal{N}_m$ around voxel *m* in the DW-MRI image (**N**). We then normalize the similarity values using the similarity values between block *m* and all the blocks in $\mathcal{N}_m$,

$$s_j = \frac{\mathrm{SCC}_j}{\sum_k \mathrm{SCC}_k} \quad (1)$$

We use the squared cross correlation (scc) as the similarity measure between each pair of blocks, because of the intensity difference between corresponding anatomical areas in two image modalities. s_j is the normalized similarity between block *m* in **M** and block *j* in $\mathcal{N}_m$.

To register two images, we find a dense transformation vector field *T* applied to image **N** to align it with image **M.** For each block *m*, we find a transformation that maximizes probability of blocks in $\mathcal{N}_m$ being matched to block *m*, that is,

$$p(m, C|\mathcal{N}_m, T) = \prod_j \left[p(C_j = 1)p(m|n_j, T)\right]^{A_j} \quad (2)$$

where C is a binary hidden random variable representing most likely a-posteriori match between two blocks in two images such that $\mathrm{C}_j = 1$ shows a complete match, and $\mathrm{C}_j = 0$ shows no match. Likewise, A is a binary variable illustrating our *prior* knowledge for matching two blocks such that $p(A_j = 1) = s_j$. Last, $p(m|n_j, T)$ represents the probability of two blocks being matched using the geometric information based on the distance between two block centers m and n_j in **M** and $\mathcal{N}_m$.

We solve this problem using the Expectation-Maximization algorithm. We iteratively update the matches by maximizing the following function that uses the similarity metric together with the geometric information [9],

$$\arg\max_T \mathbf{E_C}\left[\log\left(p(m, C|\mathcal{N}_m, T^{(t)})\right)|T^{(t-1)}\right] \quad (3)$$

The above equation can be expanded as,

$$\arg\max_T \sum_j p(C_j = 1)\left(\log p(m|n_j, T)\right) \quad (4)$$

Considering a Gaussian probability for $p(m|n_j, T)$, we obtain:

$$\arg\min_T \sum_j p(C_j = 1)\left\|T \circ m - n_j\right\|^2 \quad (5)$$

We iteratively update the block-pair matching probability, $p(\mathrm{C}_j = 1)$, using the distance between two blocks at E-step, and then update the transformation based on the updated probability at M-Step (Table 1). To accelerate the convergence, we remove the blocks with low matching values by setting $s_j = 0$.

Table 1. The Expectation-Maximization process to update the matches C, and estimate the transformation T.

Input: **M** and **N**
Output: Dense field transformation T
Initialization: $s_j \leftarrow$ Block Matching process (**M**, **N**) $T^{(0)}$: identity transformation
E-Step [9]: $p(C_j = 1) = \frac{s_j\, p(m|n_j, T^{(t-1)})}{\sum_k s_k\, p(m|n_k, T^{(t-1)})}$
M-Step: $\arg\min_{T^{(t)}} \sum_j p(C_j = 1)\left\|T^{(t)} \circ m - n_j\right\|^2$

The estimated deformation is a dense vector field illustrating the translation at each point. We use a Gaussian smoothing filter (σ^2=5) to regularize the estimated deformation field (*T*) at each iteration.

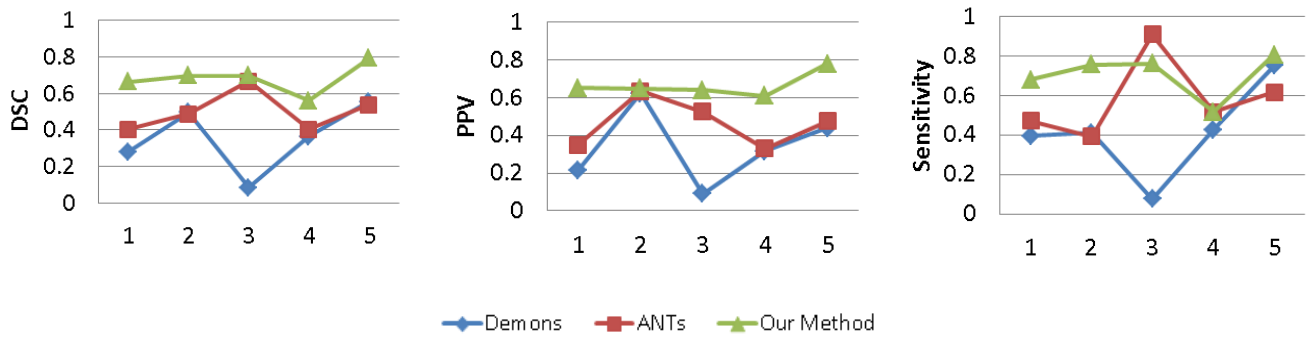

(a) (b) (c)

Fig. 2. (a) Dice coefficient score, (b) PPV, and (c) sensitivity of our method, ANTS and Demons among all five CD subjects.

3. RESULTS

To examine the segmentation performance, we measure Dice Similarity Coefficient (DSC) [10],

$$\mathrm{DSC}(A,B) = \frac{2|A \cap B|}{|A|+|B|}$$

where A and B illustrate the segmentation of the DW-MRI image after application of registration and the ground truth manual segmentation of the T1 image respectively. We also measure positive predictive value (PPV) as the probability of correct recognition of the labels, and sensitivity as the probability of correct recognition of all the ground truth labels, which are defined as follows:

$$\mathrm{PPV} = \frac{\mathrm{T_P}}{\mathrm{T_P}+\mathrm{F_P}}$$

and,

$$\mathrm{Sensitivity} = \frac{\mathrm{T_P}}{\mathrm{T_P}+\mathrm{F_N}}$$

where $\mathrm{T_P}$, $\mathrm{F_N}$ and $\mathrm{F_P}$ are true positive, false negative and false positive, respectively.

3.1. Comparison with Different Registration Algorithms

We measured our registration performance and compared it to two state-of-the-art registration methods (i.e., ANTS [11] and Demons [12]) on five CD datasets as mentioned above. We set the block size=7×7×7, and the neighborhood size=11×11×11. Figure 2 shows the performance of our method in comparison to other methods for each of the five subjects separately. The Dice scores, PPV and Sensitivity of our method were higher than other methods in the majority of cases, which illustrates better performance of our method.

Further, as illustrated in Table 2, dice score average of our method was higher than other methods, and the dice score standard deviation of our method was smaller than other methods across all the subjects. Our method shows 26% and 48% improvement in the average of dice score values compared with ANTS and Demons, respectively. Regarding the average manually segmented bowel wall volume of the CD subjects, a 1% difference between Dice coefficients accounts for an estimated 90 voxel difference between two segmentations, which means our registration method correctly registered, on average, about 2,500 voxels, and significantly outperformed the other registration methods.

Table 2. Mean and standard deviation (mean±SD) of Dice score, PPV and sensitivity for the CD subjects achieved by three registration methods

	Our method	Demons	ANTS
DSC	0.6823±0.0832	0.3553±0.1866	0.4985±0.1100
PPV	0.6654±0.0655	0.3372±0.2054	0.4622±0.1265
Sensitivity	0.7048±0.1137	0.4127±0.2390	0.5825±0.2004

Figure 3 shows the whole-body T1w structural images before and after contrast injection along with DW-MRI image (b=800 s/mm^2) and Apparent Diffusion Coefficient (ADC) map generated from the acquired DW-MR images. The manually segmented enhanced bowel wall has been circled in red in the images. The thickened CD region of the bowel wall can be distinguished in post contrast T1w (Fig 3b), which can also be recognized in the ADC map with lower intensity, and in the DW-MRI with higher intensity compared to surrounding areas. Therefore, the radiologists can easily overlay different image modalities, identify the CD region in the ADC map, and find its corresponding anatomic region in T1w.

3.2. Execution Time

Table 3 illustrates the execution time of each registration algorithm computed over five subjects. Note that the presented registration times do not include the rigid registration time, which was applied to the images before non-rigid registration to bring them into a rigid alignment. The execution time of ANTS was the longest among them.

Table 3. Execution time: Mean±SD (min)

	Our method	ANTS	Demons
Time	20.54±0:18	42.29±5.97	5.51±0.02

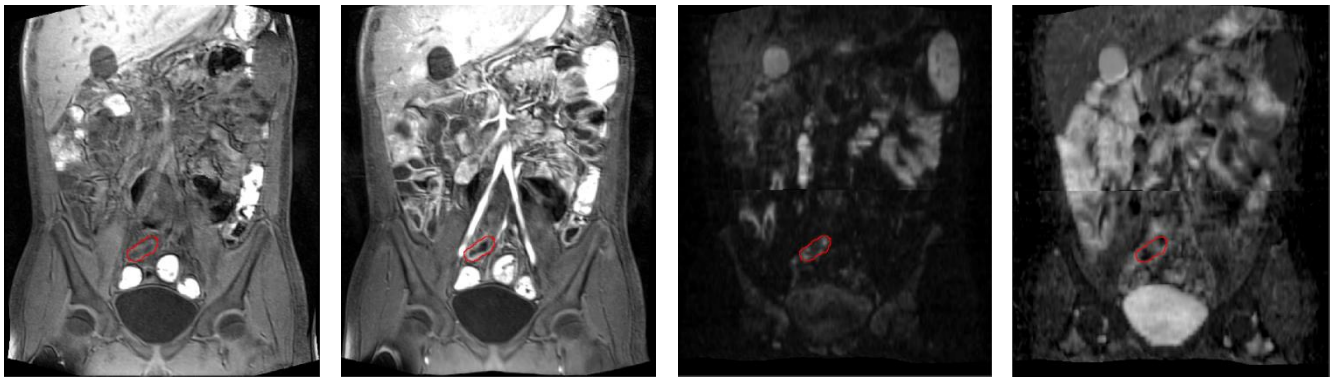

(a) (b) (c) (d)

Fig. 3. The whole-body T1w structural images (a) before and (b) after contrast injection along with (c) DW-MRI image (b=800 s/mm^2) and (d) ADC map generated from the acquired DW-MR images from coronal and axial views. The manually segmented enhanced bowel wall has been circled in red in the images.

4. CONCLUSION

This study proposes a registration method to bring structural T1w and DW-MR images into alignment. This problem is of utmost importance, as CD regions can be easily localized in the DW-MR parameter maps, yet identifying their corresponding anatomic areas in the T1w image is challenging, due to lower DW-MR resolution and lower signal-to-noise ratio. The proposed registration method makes the fusion of the information from the T1w and DW-MR images possible, and simplifies the integration of the information extracted from DW-MRI for fast and accurate diagnosis and severity assessment. Our method has been tested on patients with confirmed CD in the bowel. The accuracy of our method has been compared with other registration methods in the literature, i.e. ANTS and Demons, and outperformed them.

5. ACKNOWLEDGEMENTS

This research is supported in part by the National Institute of Diabetes & Digestive & Kidney Diseases of the National Institutes of Health under award number R01DK100404.

6. REFERENCES

[1] A. Oto, *et al.*, "Evaluation of diffusion-weighted MR imaging for detection of bowel inflammation in patients with Crohn's disease," *Academic radiology*, vol. 16, pp. 597-603, 2009.

[2] R. Kaewlai and H. Abujudeh, "Nephrogenic systemic fibrosis," *American Journal of Roentgenology*, vol. 199, pp. W17-W23, 2012.

[3] H. Neubauer, *et al.*, "Small-bowel MRI in children and young adults with Crohn disease: retrospective head-to-head comparison of contrast-enhanced and diffusion-weighted MRI," *Pediatric radiology*, vol. 43, pp. 103-114, 2013.

[4] S. Kurugol, *et al.*, "Spatially-Constrained Probability Distribution Model of Incoherent Motion (SPIM) in Diffusion Weighted MRI Signals of Crohn's Disease."

[5] V. Taimouri, *et al.*, "Spatially Constrained Incoherent Motion (SCIM) model improves quantitative Diffusion-Weighted MRI analysis of Crohn's disease patients," in *Abdominal Imaging. Computation and Clinical Applications*, ed: Springer, 2013, pp. 11-19.

[6] M. Erdt, S. Steger, and S. Wesarg, "Deformable registration of MR images using a hierarchical patch based approach with a normalized metric quality measure," in *Biomedical Imaging (ISBI), 2012 9th IEEE International Symposium on*, 2012, pp. 1347-1350.

[7] P. A. Yushkevich, *et al.*, "User-guided 3D active contour segmentation of anatomical structures: significantly improved efficiency and reliability," *Neuroimage*, vol. 31, pp. 1116-1128, 2006.

[8] S. Ourselin, *et al.*, "Block matching: A general framework to improve robustness of rigid registration of medical images," in *Medical Image Computing and Computer-Assisted Intervention–MICCAI 2000*, 2000, pp. 557-566.

[9] S. Granger and X. Pennec, "Multi-scale EM-ICP: A fast and robust approach for surface registration," *Lecture notes in computer science*, pp. 418-432, 2002.

[10] L. R. Dice, "Measures of the amount of ecologic association between species," *Ecology*, vol. 26, pp. 297-302, 1945.

[11] B. B. Avants, *et al.*, "Symmetric diffeomorphic image registration with cross-correlation: evaluating automated labeling of elderly and neurodegenerative brain," *Medical image analysis*, vol. 12, pp. 26-41, 2008.

[12] T. Vercauteren, *et al.*, "Diffeomorphic demons: Efficient non-parametric image registration," *Neuroimage*, vol. 45, pp. S61-S72, 2009.